



ELSEVIER

23 April 2001

Physics Letters A 282 (2001) 235–244

PHYSICS LETTERS A

www.elsevier.nl/locate/pla

Production of two-Fock states superpositions from even circular states and their decoherence

A.L. Souza Silva^{a,1}, W. Duarte José^b, V.V. Dodonov^{a,*}, S.S. Mizrahi^a

^a Departamento de Física, CCET, Universidade Federal de São Carlos, Rod. Washington Luiz km 235, São Carlos, 13565-905, SP, Brazil

^b Departamento de Ciências Exatas e Tecnológicas, Universidade Estadual de Santa Cruz, Rod. Ilhéus-Itabuna km 16, Ilhéus, BA, Brazil

Received 23 February 2001; accepted 9 March 2001

Communicated by V.M. Agranovich

Abstract

We analyze the even circular state (ECS — a superposition of N coherent states $|\alpha\rangle$ uniformly distributed with equal amplitudes on a circle) that can be engineered for the center of mass vibrational motion of a trapped ion. As a result of interference effects in phase space this state shows interesting features: depending on the value of $|\alpha|$ it may show up as the vacuum state $|0\rangle$, the number state $|N\rangle$ or as two-state superposition, $|0\rangle + |N\rangle$, $|N\rangle + |2N\rangle$. Here we discuss the statistics of the ECS, the probability for its production, its evolution under the effects of the environment and decoherence. © 2001 Published by Elsevier Science B.V.

PACS: 42.50.Vk; 42.50.Ct; 32.90.+a; 03.65.Bz

Keywords: Even circular states; Trapped ion; Decoherence; Relaxation

1. Introduction

Engineering of quantum states [1] that do not exist in the natural world is an exciting problem of nowadays quantum mechanics and recent advances in quantum optics have allowed the realization of this challenge with much success. A variety of states have been produced already, both for the modes of electromagnetic field in QED superconducting cavities [2] and for the vibrational modes of trapped ions [3]. They include, in particular, squeezed states and different

kinds of the “Schrödinger cat” states. An interesting problem is the generation of the “most nonclassical” Fock states $|n\rangle$ and their finite superposition, such as $|n_1\rangle + |n_2\rangle$. Many different schemes have been proposed for this purpose [4]. In this Letter, we consider the possibilities of constructing the Fock states via the so-called *circular states* [5],

$$|\Psi_N(\alpha_0)\rangle = \sum_{k=1}^N C_k |\alpha_k\rangle, \quad \alpha_k = \alpha_0 e^{i2\pi k/N}, \quad (1)$$

where the coherent-states components are given by

$$|\alpha_k\rangle = e^{-|\alpha_k|^2/2} \sum_{n=0}^{\infty} \frac{\alpha_k^n}{\sqrt{n!}} |n\rangle.$$

For the first time the superposition of N harmonic oscillator coherent states $|\alpha_k\rangle$ (having same modulus $|\alpha_k| \equiv \sqrt{a}$ and uniformly distributed along a circle of

* Corresponding author.

E-mail addresses: palus@df.ufscar.br (A.L. Souza Silva), wjose@jacaranda.uesc.br (W. Duarte José), vdodonov@df.ufscar.br (V.V. Dodonov), salomon@df.ufscar.br (S.S. Mizrahi).

¹ On leave from Universidade Federal de Rondônia, Brazil.

radius \sqrt{a} in the phase space $\{\text{Re}\alpha, \text{Im}\alpha\}$ have been considered in [6]. The difference between the states introduced in [6] and in [5] is in the “weights” of each coherent state in the superposition. In [6] these weights were chosen different, in order to ensure the *Poissonian* photon statistics, whereas in the case of circular states considered in [5], all the coefficients have the same absolute value, resulting in non-Poissonian statistics. The case of $N = 2$ with $C_2 = \pm C_1$ was studied in [7], where the name “even and odd coherent states” has been introduced. The superposition of two coherent states resulting in exact Poissonian statistics have been considered in [8]. During the last decade, superposition of coherent states attracted much attention due to their interference in phase space, leading to nonclassical properties as antibunching or sub-Poissonian statistics, squeezing, etc. In particular, the results of studies of different kinds of the circular states and their generalizations have been reported in [9–11]. Experimental schemes permitting to generate such superpositions were proposed in [12] (for the electromagnetic field in superconducting cavities) and in [13,14] (for the vibrational states of the center of mass of a trapped ion).

As shown in [12], an arbitrary quantum state can be approximated by a superposition of coherent states located on a circle in phase space. One state that shows particularly interesting properties is the *even circular state* (ECS), which has equal amplitudes of all coherent components: $C_1 = C_2 = \dots = C_N$. As a result of interference effects, this state shows interesting features: depending on the value of $|a|$ it may show up, very closely, as the vacuum state $|0\rangle$, the number state $|N\rangle$ or as a superposition of two Fock states, $|jN\rangle + |(j+1)N\rangle$, $j = 0, 1, 2, \dots$

In this Letter we analyze the properties of the ECSs. In particular, we are interested in the case when the phase space interference reduces the ECS to the superposition of two Fock states differing by an appreciable quantity of quanta, $|0\rangle + |N\rangle$ and $|N\rangle + |2N\rangle$. Basing on the results of Ref. [14], we give the probability for producing (with appropriate interactions with laser beams) such states for the center of mass motion of a vibrational ion.

Many authors studied the influence of an environment on the stability of the superposition of quantum states [15]. It was shown that the off-diagonal terms in the density operator, expressed in a coherent-state ba-

sis, are weighted with a time-dependent factor which rapidly eliminates the coherence, so that macroscopic superpositions are reduced to statistical mixtures very rapidly (usually, the name “decoherence” is used for this process). Recently [16], we have introduced a specific parameter \mathcal{C} which gives a quantitative measure of the degree of coherence in terms of the coefficients ρ_{mn} of the density matrix in the Fock-state basis. This parameter varies between 1 for pure quantum states and 0 for thermalized equilibrium states. Writing the Wigner function for the ECS, we give its time evolution under the effect of the environment and compare the *purity* and the coherence parameter in their route to thermal relaxation.

This Letter is organized as follows. In Section 2 we analyze the properties of the ECS and the possibility to engineer two-Fock states for the center of mass vibrational motion of a trapped ion. In Section 3 we discuss the quantitative measure of (de)coherence and consider the time evolution of the ECSs under the influence of a thermal environment. The final Section 4 is devoted to summary and conclusions.

2. Even circular states

For N even and $C_{k+N/2} = \pm C_k$ the parity of state (1) may be even or odd, i.e., $|\Psi_N(-\alpha_0)\rangle = \pm |\Psi_N(\alpha_0)\rangle$. Any circular state is also an eigenstate of the N th power of the annihilation operator, $\hat{a}^N \times |\Psi_N(\alpha_0)\rangle = \alpha_0^N |\Psi_N(\alpha_0)\rangle$, belonging therefore to a wide family of the “ N -photon” states [17]. The particular ECS with $C_1 = C_2 = \dots = C_N$ proposed in [5] (now on we call it as N-ECS) can be represented in two equivalent normalized forms:

$$|\tilde{\Psi}_N(a)\rangle = A_N^{1/2} \sum_{k=1}^N |\alpha_k\rangle = \tilde{A}_N^{1/2} \sum_{j=0}^{\infty} \frac{a^{Nj/2}}{\sqrt{(Nj)!}} |Nj\rangle, \quad (2)$$

where

$$\alpha_k = \sqrt{a} \exp(2i\varphi_k), \quad \varphi_k = \pi k/N, \quad (3)$$

$$A_N^{-1} = N + 2 \sum_{k=0}^{N-1} k \exp[-2a \sin^2(\varphi_k)] \times \cos[a \sin(2\varphi_k)], \quad (4)$$

$$\tilde{A}_N^{-1} = \sum_{k=0}^{\infty} \frac{a^{Nk}}{(Nk)!}, \quad \tilde{A}_N = N^2 e^{-a} A_N. \quad (5)$$

So, for a given N , state (2) is a superposition of the Fock states $|Nj\rangle$ with $j = 0, 1, 2, \dots$

The photon number probability of the N-ECS is

$$P_n(N, a) = |\langle n | \tilde{\Psi}_N \rangle|^2 = \tilde{A}_N \frac{a^{Nj}}{(Nj)!} \delta_{n, Nj}. \quad (6)$$

The mean value for any power of \hat{n} can be calculated as

$$\overline{n^k} = \sum_{n=0}^{\infty} n^k P_n = \tilde{A}_N N^k \sum_{j=0}^{\infty} \frac{a^{Nj} j^k}{(Nj)!}. \quad (7)$$

Other quantities that characterize the field statistics are the variance $\text{Var}(\hat{n}) \equiv \overline{n^2} - (\bar{n})^2$ and the Mandel parameter [18], $Q \equiv (\text{Var}(\hat{n}) - \bar{n})/\bar{n}$. For $Q < 0$ the field has a sub-Poissonian statistics, for $Q = 0$ the statistics is Poissonian and for $Q > 0$ the statistics is super-Poissonian.

As shown in [9], taking the superposition of $N + 1$ coherent states in form (1) with the coefficients $C_k = \exp[2\pi ik/(N + 1)]$, one obtains the state close to the Fock state $|N\rangle$, if $|\alpha_0| \ll 1$. This is a generalization of the *odd coherent state* [7], whose limit at $|\alpha_0| \rightarrow 0$ is the first excited Fock state $|1\rangle$. In our Letter, we consider the case of *large* coherent state amplitudes $|\alpha_0|$ and equal coefficients C_k . If $N \gg 1$ and j is not very large, then only one or two terms of expansion (2) over the Fock basis are essential, whereas the contributions of all other terms are extremely small, due to rapidly growing factorial terms $(Nj)!$ in denominators. For $(ea/N)^N \ll 1$ we have the set of “approximate vacuum states” $|\tilde{0}\rangle$, all of which are close to the true vacuum state $|0\rangle$ [11]. In the true vacuum state the parameter Q is not defined, however $|\tilde{0}\rangle$ possesses highly super-Poissonian statistics, and in the limit $a \rightarrow 0$ one has $Q \rightarrow N$ [11]. Increasing the value of a , one arrives at a family of “approximate number states” $|\tilde{N}\rangle$, each member of which is close to the true number state $|N\rangle$, provided parameter a belongs to the interval $1 \ll (ea/N)^N \ll 4^N$. Such “approximate single-Fock states” have been studied in [11].

2.1. Special even circular states

Here we consider the case when the finite coherent state superposition (2) is reduced effectively to the “two-Fock state”

$$|\Psi_{N,j}\rangle = (\xi^2 + 1)^{-1/2} (|Nj\rangle + \xi |N(j + 1)\rangle), \quad (8)$$

where ξ may be any positive number (although not very different from 1, say, in the interval $10^{-1} \leq \xi \leq 10$, because, e.g., for $\xi = 10$ the weight of the state $|Nj\rangle$ in superposition (8) is only 1%, and this superposition becomes effectively the “single-Fock state” $|N(j + 1)\rangle$).

By setting the value of the parameter a equal to either of

$$\gamma_j = \{\xi^2 [N(j + 1)]! / (Nj)!\}^{1/N}, \quad j = 0, 1, 2, \dots, \quad (9)$$

one can equalize the ratio of the coefficients of two subsequent Fock states, $|N(j + 1)\rangle$ and $|Nj\rangle$ in (2), to any desired positive number ξ . Then, if $N \gg 1$ each state $|\tilde{\Psi}_N(\gamma_j)\rangle \equiv |\tilde{\Psi}_{N,j}\rangle$ comes very close to state (8). Therefore, the special circular states with $N \gg 1$ can mimic, in some sense, two-level systems. The level separation can be regulated by the choice of the oscillator frequency ω and the number of interfering coherent states N . (Note that the superpositions of the first two number states, $|0\rangle$ and $|1\rangle$, have been studied in [19] under the name *Bernoulli states*; see also [20].)

For example, for $a = \gamma_j$ and $\xi = 1$ state (2) comes close to the “symmetric two-Fock state” (STFS) $2^{-1/2}(|Nj\rangle + |N(j + 1)\rangle)$. For $j = 0$ and $a \approx N/e$ we obtain the superposition $|\tilde{\Psi}_{N,0}\rangle \approx (|0\rangle + |N\rangle)/\sqrt{2}$, for $j = 1$ and $a \approx 4N/e$ we have the superposition $|\tilde{\Psi}_{N,1}\rangle \approx (|N\rangle + |2N\rangle)/\sqrt{2}$, and so on. Such a sequence of “single-Fock states” and “two-Fock states” is clearly seen in Fig. 1, where we plot the dependence of difference $\text{Var}(\hat{n}) - \bar{n}$ on parameter a , for $N = 8, 16$. For $0 < a \lesssim 2$ ($N = 8$) and $0 < a \lesssim 4$ ($N = 16$) the approximate vacuum-state $|\tilde{0}\rangle \approx |0\rangle$ results. Maxima correspond to the “approximate symmetrical two-Fock states”, $|\tilde{\Psi}_{N,j}\rangle$, $j = 0, 1, 2$ for the first, second, third maximum, respectively, further maxima will depart more significantly from the two-Fock states. The first minima correlate with the “approximate single-Fock states”, $|\tilde{\Psi}_8(a = 6.80)\rangle \approx |8\rangle$ and $|\tilde{\Psi}_{16}(a = 12.8)\rangle \approx |16\rangle$.

For $a = \gamma_j$ in (2) the overlap $P_{N,j} \equiv |\langle \Psi_{N,j} | \tilde{\Psi}_{N,j} \rangle|^2$ between the approximate two-Fock state $|\tilde{\Psi}_{N,j}\rangle$ and its exact STFS partner $(|Nj\rangle + |N(j + 1)\rangle)/\sqrt{2}$ (hereafter we confine ourselves to the symmetric case $\xi = 1$) is very close to 1, if j is small. For example, in the case of $j = 0$, using Stirling’s asymptotic formula for the factorials, we have $P_{N,0} \approx 1 - 2^{-2N-1} \sqrt{\pi N}$. The mean photon number in the superposition $|\tilde{\Psi}_{N,j}\rangle$

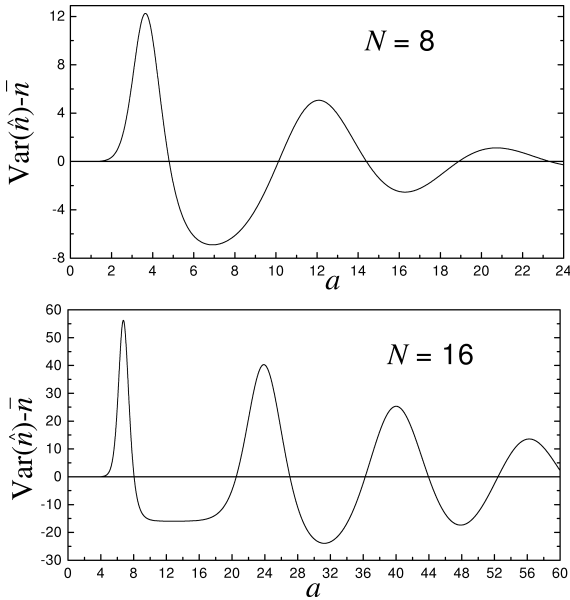


Fig. 1. $\text{Var}(\hat{n}) - \bar{n}$ as a function of a for the even circular states with $N = 8, 16$.

is close to $N(2j + 1)/2$, and the variance $\text{Var}(\hat{n}) \approx N^2/4$ is independent of j . The Mandel parameter equals $Q \approx N[2(2j + 1)]^{-1} - 1$. The statistics is sub-Poissonian only for $N < 2(2j + 1)$, but it is super-Poissonian for N sufficiently large. For instance, the state $(|10\rangle + |20\rangle)/\sqrt{2}$ has a super-Poissonian statistics, whereas that of state $(|4\rangle + |8\rangle)/\sqrt{2}$ is sub-Poissonian.

A good coincidence of the heights of the maxima in Fig. 1 with the ideal dependence $\text{Var}(\hat{n}) - \bar{n} = N^2/4 - Nj - N/2$ is observed only for $j = 0, 1$ if $N = 8$ and $j = 0, 1, 2$ if $N = 16$. For larger values of j we see some deviations, especially for $N = 8$. As to the single-Fock states, only the state $|N\rangle$ is well approximated by the N-ECS, whereas the states $|2N\rangle$ and $|3N\rangle$ can be approximated with smaller overlaps (for $N = 16$ and especially for $N = 8$). The greater is the number N of interfering coherent components in (2), more single-Fock and two-Fock states can be approximated by the N-ECS.

A rough estimation of the optimal values of γ_j (Eq. (9)) for $j > 1$ (and $\xi = 1$) is $\gamma_j \approx (N/e)(j + 1)^{j+1}/j^j$, which goes to $\gamma_j \approx Nj$ for $j \gg 1$. This means that even circular states with $a \sim Nj$ give a good approximation for the “single-Fock states” only

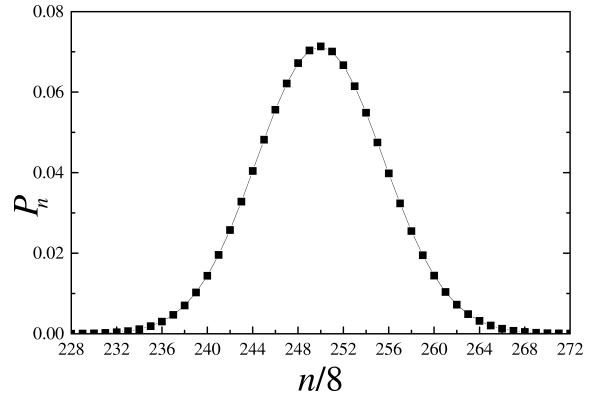


Fig. 2. Probability distribution P_n as function of $j = n/N$ for $N = 8$ and $a = 2000$.

if j is of the order of 1. The range of values of a for obtaining the “two-Fock states” is wider, although it is also finite: calculating the ratio of coefficients of terms $|N(j + 2)\rangle |N(j + 1)\rangle$ in (2), for $a = \gamma_j$ one obtains the factor $\exp(-N/j)$ for $N \gg 1$ and $j \gg 1$. Consequently, the total number of possible “two-Fock states” which can be approximated by N-ECS does not exceed N . As one increases the value of a the number of Fock states that contribute significantly to the probability distribution P_n ($n \equiv Nj$) increases, as can be seen in Fig. 2, where we assumed $N = 8$ and $a = 2000$.

2.2. Generation of special states for the vibrational CM motion of a trapped ion

In [14] it was shown that the N-ECSs with $N = 2^M$ can be produced for the vibrational CM motion of a trapped ion, by a sequence of M laser pulses tuned resonantly with the electronic transition frequency. After each laser pulse the ion electronic state is determined by one fluorescence measurement, which should be negative (fluorescence absence) for the process to proceed successfully. So, the probability of getting the required ion vibrational state (2) is

$$P_{\uparrow}(a) = 2^{-2M} [A_{2M}]^{-1}, \quad (10)$$

where A_{2M} is given by (4) with $N = 2^M$. In Fig. 3 we plotted the estimated probability P_{\uparrow} as function of a for $M = 3$ (solid line: superposition of 8 coherent states) and $M = 4$ (dashed line: superposition of 16 coherent states), the arrows point to the values of a

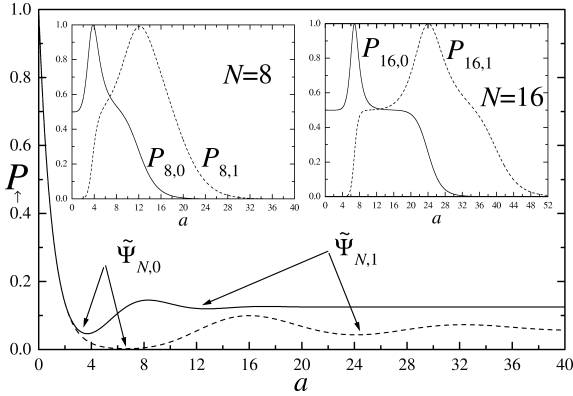


Fig. 3. Probability for producing a circular even state $|\tilde{\Psi}_N\rangle$ with $N = 2^M$ for a trapped ion after M successful cycles as function of $a = |\alpha_0|^2$. The order of the curves from top to bottom: $M = 3$ (solid line) and $M = 4$ (dashed line). In the insertions: the overlap $P_{N,j} \equiv |\langle \Psi_{N,j} | \tilde{\Psi}_{N,j} \rangle|^2$ between the “approximate two-Fock state” $|\tilde{\Psi}_{N,j}\rangle$ and its exact STFS partner $|\Psi_{N,j}\rangle = (|Nj\rangle + |N(j+1)\rangle)/\sqrt{2}$ versus a for $N = 8$ and $N = 16$ (solid lines $P_{N,0}$ and dashed lines $P_{N,1}$).

that lead to the special states $|\tilde{\Psi}_{N,j}\rangle$. In the insertions we plotted the overlaps between the exact and approximate two-Fock states, $P_{N,j} \equiv |\langle \Psi_{N,j} | \tilde{\Psi}_{N,j} \rangle|^2$, for $j = 0$ and $j = 1$, versus a for $N = 8$ and $N = 16$. The sets of values $S = \{N, a = \gamma_j\}$ satisfying condition (9), necessary for the N-ECS coming close to state $|\Psi_{N,0}\rangle$ are $S = \{8, 3.76\}$ and $S = \{16, 6.8\}$, respectively (first maxima in Fig. 1). For $j = 1$ the N-ECS comes close to $|\Psi_{N,1}\rangle$ for $S = \{8, 12.17\}$ and $S = \{16, 24.1\}$, respectively (second maxima in Fig. 1). The probability for producing the state $|\tilde{\Psi}_{8,0}\rangle$ in the trap (using the scheme of [14]) is about 4.5% ($a = 3.76$) while the state $|\tilde{\Psi}_{8,1}\rangle$ has a higher probability, 12.8% ($a = 12.17$). These values for a in Fig. 3 occur near the first minima (10) of the curves, being lower for $|\tilde{\Psi}_{8,0}\rangle$ than for $|\tilde{\Psi}_{8,1}\rangle$. The same occurs for $N = 16$ but with lower probabilities, meaning that it is harder to produce a two-Fock state containing the vacuum state ($|\tilde{\Psi}_{N,0}\rangle$), than to produce the superposition of $|N\rangle$ and $|2N\rangle$ ($|\tilde{\Psi}_{N,1}\rangle$).

In Table 1 we present a summary of our results, where $P \equiv P_{N,j}$ (for the single-Fock states $|8\rangle$ and $|16\rangle$), the values of P and the sets (N, a) correspond to the maximal values of the overlaps between the exact wave functions and their N-ECS approximations).

3. Relaxation and decoherence

3.1. The measure of “coherence”

Since “decoherence” is usually identified with the disappearance, with time progression, of the *off-diagonal elements* of the density matrix $\hat{\rho} = \sum_{mn} \rho_{mn} \times |m\rangle\langle n|$ in a given basis, it was proposed in [16] to use the ratio

$$\mathcal{C}(t) = \frac{\sum_{m \neq n} |\rho_{mn}|^2(t)}{\sum_{m \neq n} |\rho_{mn}|^2(0)} \quad (11)$$

as the quantitative measure characterizing the rate of decoherence in the Fock-state basis. Evidently, $\mathcal{C}(0) = 1$, while $\mathcal{C} \equiv 0$ for any “completely incoherent” state without off-diagonal matrix elements in the energy basis (provided initially at least one off-diagonal element was different from zero). Introducing the “diagonal part” of the operator $\hat{\rho}$,

$$\hat{\rho}_d = \sum_n P_n |n\rangle\langle n|, \quad P_n \equiv \langle n | \hat{\rho} | n \rangle, \quad (12)$$

and taking into account the property $\text{Tr}(\hat{\rho}\hat{\rho}_d) = \text{Tr}(\hat{\rho}_d^2)$ one can rewrite (11) in the form

$$\mathcal{C} = \frac{\text{Tr}[\hat{\rho}(t) - \hat{\rho}_d(t)]^2}{\text{Tr}[\hat{\rho}(0) - \hat{\rho}_d(0)]^2} \equiv \frac{\mu(t) - \lambda(t)}{\mu(0) - \lambda(0)}, \quad (13)$$

where we defined

$$\mu \equiv \text{Tr} \hat{\rho}^2, \quad \lambda \equiv \text{Tr} \hat{\rho}_d^2 = \sum_n P_n^2. \quad (14)$$

We shall call μ the “total purity” and λ the “diagonal purity”. In many cases of practical interest both “purities” can be calculated rather easily. For example, if one knows the *Wigner function* [21] (we assume $\hbar \equiv 1$)

$$W(q, p, t) = \int dv e^{ipv} \left\langle q - \frac{v}{2} \left| \hat{\rho} \left| q + \frac{v}{2} \right. \right. \right\rangle,$$

$$\text{Tr} \hat{\rho} = \int W(q, p) dq dp / (2\pi) = 1, \quad (15)$$

then

$$\mu = \int W^2(q, p) dq dp / (2\pi). \quad (16)$$

The occupation probabilities $P_n(t)$ (the photon distribution function) necessary for calculating the “diagonal purity”, can be also expressed through the Wigner

Table 1

Special even circular states	(N, a)	P	$P_{\uparrow}(a)$	\bar{n}	$\text{Var}(\hat{n})$
$ \tilde{\Psi}_{8,0}\rangle \approx (0\rangle + 8\rangle)/\sqrt{2}$	(8, 3.76)	0.999960	0.04635	4.00322	16.00497
$ \tilde{\Psi}_8^{(1)}\rangle \approx 8\rangle$	(8, 6.80)	0.982674	0.12851	7.99994	1.10908
$ \tilde{\Psi}_{8,1}\rangle \approx (8\rangle + 16\rangle)/\sqrt{2}$	(8, 12.17)	0.991848	0.12016	11.94293	16.99720
$ \tilde{\Psi}_8^{(2)}\rangle \approx 16\rangle$	(8, 15.80)	0.79002	0.12542	15.99847	13.62115
$ \tilde{\Psi}_{16,0}\rangle \approx (0\rangle + 16\rangle)/\sqrt{2}$	(16, 6.80)	0.999999	0.00261	7.99560	63.99998
$ \tilde{\Psi}_{16}^{(1)}\rangle \approx 16\rangle$	(16, 12.80)	0.999918	0.08564	16.00001	0.02088
$ \tilde{\Psi}_{16,1}\rangle \approx (16\rangle + 32\rangle)/\sqrt{2}$	(16, 24.10)	0.999807	0.04295	24.12047	64.05677
$ \tilde{\Psi}_{16}^{(2)}\rangle \approx 32\rangle$	(16, 31.20)	0.96834	0.07190	32.02314	8.10407

The first column stands for the particular states coming out from a N-ECS, due to interference in phase space; the second column gives the corresponding pairs of values (N, a) to be attributed to the N-ECS; the third column stands for the maximum probability of a particular state in the N-ECS; the fourth column shows the probability for the experimental production of a particular state for the ion CM vibrational motion; finally, fifth and sixth columns give the corresponding mean numbers and photon variances.

function as [21]

$$P_n(t) = \frac{1}{2\pi} \int W(q, p, t) W_n(q, p) dq dp, \quad (17)$$

where $W_n(q, p)$ is the Wigner function (with dimensionless variables) for the number state $\hat{\rho} = |n\rangle\langle n|$, which can be expressed either in terms of the Laguerre polynomials [21,22],

$$W_n(q, p) = 2(-1)^n \exp[-(q^2 + p^2)] \times L_n(2[q^2 + p^2]),$$

or through the products of the Hermite polynomials [23],

$$W_n(q, p) = 2^{-2n+1} \exp[-(q^2 + p^2)] \times \sum_{j=0}^n \frac{1}{j!(n-j)!} H_{2j}(\sqrt{2}q) \times H_{2(n-j)}(\sqrt{2}p). \quad (18)$$

We used in calculations representation (18).

3.2. Time evolution of the even circular states

We assume that the relaxation process due to the interaction with some thermal environment can be described in the framework of the standard master

equation [24]

$$d\hat{\rho}/dt = \gamma(1 + \nu)(2\hat{a}\hat{\rho}\hat{a}^\dagger - \hat{a}^\dagger\hat{a}\hat{\rho} - \hat{\rho}\hat{a}^\dagger\hat{a}) + \gamma\nu(2\hat{a}^\dagger\hat{\rho}\hat{a} - \hat{a}\hat{a}^\dagger\hat{\rho} - \hat{\rho}\hat{a}\hat{a}^\dagger) - i[\hat{a}^\dagger\hat{a}, \hat{\rho}], \quad (19)$$

where ν is the equilibrium mean number of quanta in the reservoir corresponding to the given mode, and $\gamma > 0$ is a damping coefficient ($\hbar = \omega = 1$). Eq. (19) is equivalent to the Fokker–Planck equation for the time-dependent Wigner function $W(q, p, t)$:

$$\frac{\partial W}{\partial t} = \frac{\partial}{\partial q}([\gamma q - p]W) + \frac{\partial}{\partial p}([\gamma p + q]W) + \gamma \left(\nu + \frac{1}{2} \right) \left(\frac{\partial^2 W}{\partial q^2} + \frac{\partial^2 W}{\partial p^2} \right). \quad (20)$$

Applying the propagator of Eq. (20), obtained in [16], to the initial Wigner function, after some algebra we find the explicit expression for $W(q, p, t)$ in the form

$$W(q, p, t) = 2A_N \xi_\nu e^{-a} \sum_{k,l=1}^N \exp\left\{-\xi_\nu(q^2 + p^2) + 2\xi_\nu \sqrt{2a} e^{-\gamma t} \exp[i(\varphi_k - \varphi_l)] \times [q \cos(\varphi_k + \varphi_l - t) + p \sin(\varphi_k + \varphi_l - t)] - a[1 - 2(2\nu + 1)u\xi_\nu] \times \exp[2i(\varphi_k - \varphi_l)]\right\}, \quad (21)$$

where the phase φ_k was defined in Eq. (3), and the dependence on time in the right-hand side is contained in the functions

$$u(t) = 1 - e^{-2\gamma t}, \quad \xi_\nu(t) = [2\nu u(t) + 1]^{-1}. \quad (22)$$

Calculating integral (16) we find the “total purity”

$$\begin{aligned} \mu(N, a, u) &= A_N^2 \xi_\nu \sum_{k,l=1}^N \sum_{k',l'=1}^N \exp\{-2a + a(2\nu + 1)u\xi_\nu \\ &\quad \times (\exp[2i(\varphi_k - \varphi_l)] + \exp[2i(\varphi_{k'} - \varphi_{l'})]) \\ &\quad + 2a(1 - u)\xi_\nu \exp[i(\varphi_k + \varphi_{k'} - \varphi_l - \varphi_{l'})] \\ &\quad \times \cos(\varphi_k + \varphi_l - \varphi_{k'} - \varphi_{l'})\}. \end{aligned} \quad (23)$$

To calculate the “diagonal purity”, we obtain from Eq. (17) the photon distribution function in terms of the Laguerre polynomial of order n :

$$\begin{aligned} P_n(N, a, u) &= \frac{A_N}{\nu u + 1} \left(\frac{\nu u}{\nu u + 1} \right)^n \\ &\quad \times \sum_{k,l=1}^N \exp\left[-a \left(1 - \frac{(\nu + 1)u}{\nu u + 1} \right. \right. \\ &\quad \left. \left. \times \exp[2i(\varphi_k - \varphi_l)] \right) \right] \\ &\quad \times L_n \left(\frac{a(u - 1)}{\nu u(\nu u + 1)} \exp[2i(\varphi_k - \varphi_l)] \right). \end{aligned} \quad (24)$$

At zero temperature ($\nu = 0$) we have

$$\begin{aligned} P_n^0(N, a, u) &= \frac{A_N}{n!} e^{-a} [a(1 - u)]^n \\ &\quad \times \left\{ N e^{au} + 2 \sum_{k=0}^{N-1} k \exp[au \cos(2\varphi_k)] \right. \\ &\quad \left. \times \cos[au \sin(2\varphi_k) + 2n\varphi_k] \right\}. \end{aligned}$$

With the aid of the known series [25]

$$\begin{aligned} \sum_{n=0}^{\infty} L_n(x)L_n(y)z^n &= (1 - z)^{-1} \exp\left[z \frac{x + y}{z - 1} \right] I_0 \left[2 \frac{\sqrt{xyz}}{1 - z} \right] \end{aligned}$$

($I_0(z)$ is the modified Bessel function), the “diagonal purity” $\lambda = \sum_n P_n^2$ can be expressed as

$$\begin{aligned} \lambda(N, a, u) &= A_N^2 \xi_\nu e^{-2a} \sum_{k,l=1}^N \sum_{k',l'=1}^N \exp\{a(2\nu + 1)u\xi_\nu \\ &\quad \times (\exp[2i(\varphi_k - \varphi_l)] + \exp[2i(\varphi_{k'} - \varphi_{l'})])\} \\ &\quad \times I_0(2a(1 - u)\xi_\nu \\ &\quad \times \exp[i(\varphi_k + \varphi_{k'} - \varphi_l - \varphi_{l'})]). \end{aligned} \quad (25)$$

With respect to the evolution of the average number of photons and the higher-order moments of the photon distribution function, it is well known that in the specific case of the standard master equation (19), their values at $t > 0$ can be expressed linearly through the initial moments of lower orders, independently of the specific form of the distribution function $P_n(0)$ [26]. In particular, the first two moments evolve as follows:

$$\bar{n}(t) = \bar{n}(0)(1 - u) + \nu u, \quad (26)$$

$$\begin{aligned} \overline{n^2}(t) &= \nu u(2\nu u + 1) + (1 - u)^2 \overline{n^2}(0) \\ &\quad + u(1 - u)(1 + 4\nu)\bar{n}(0). \end{aligned} \quad (27)$$

As a consequence, we have the relation

$$\begin{aligned} [\text{Var}(\hat{n}) - \bar{n}]_t &= (1 - u)^2 [\text{Var}(\hat{n}) - \bar{n}]_{t=0} \\ &\quad + 2\nu u(1 - u)\bar{n}(0) + (u\nu)^2, \end{aligned}$$

which tells us that the kind of statistics is not changed with time in the case of zero temperature ($\nu = 0$) of the reservoir.

As shown in the preceding section, for $(ea/N) < 1$ the initial circular state is close to the vacuum state. In this case the time dependence of the “purity” has a little in common with the time dependence of the “coherence”; see Fig. 4. Similar plots for initial coherent state (with $a \sim 1$) were given in [16].

In Fig. 5 we show the evolution of “purity” and “coherence coefficient” at zero temperature for the initial approximate Fock state $|\tilde{\Psi}_8(a = 6.8)\rangle \approx |8\rangle$ and two initial approximate two-Fock states: $|\tilde{\Psi}_{8,0}(a = 3.8)\rangle \approx [|0\rangle + |8\rangle]/\sqrt{2}$ and $|\tilde{\Psi}_{8,1}(a = 12.2)\rangle \approx [|8\rangle + |16\rangle]/\sqrt{2}$. In contrast to the “purity”, the coherence coefficient is a monotonic function of time. Moreover, it decreases even more quickly than the “purity” μ (which

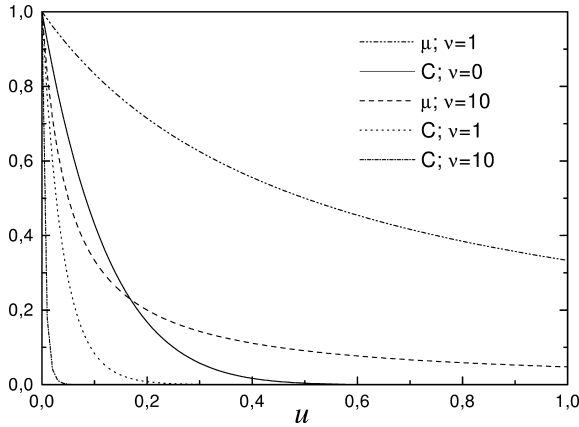


Fig. 4. The “purity” μ and the “coherence” C versus the “compact time” $u \equiv 1 - e^{-2\gamma t}$ for the initial circular state with $N = 8$, $a = 1$ and for three different temperatures. The order of the curves from top to bottom (in the left-hand side of the figure): μ for $\nu = 1$; C for $\nu = 0$ (zero temperature, in this case $\mu \equiv 1$); μ for $\nu = 10$; C for $\nu = 1$; C for $\nu = 10$.

is frequently used as a measure of decoherence; however, the use of μ for this purpose has obvious drawbacks [16], as seen clearly from the figure). The initial “rate of decoherence” is, roughly speaking, inversely proportional to the energy of quantum fluctuations in the initial state [16]. So, it is faster for $a = 12.2$ than for $a = 3.8$. An interesting feature is that after $u_1 \sim 0.2$ there is an inversion in the evolution of the coherence parameter C for different values of a , so that at the final stage of the evolution the off-diagonal elements (in the Fock basis) of the state with higher initial energy survive for a longer time than those of the states with lower initial energies.

Fig. 6 shows the “purity” and “coherence coefficient” at zero temperature as functions of a for two instants of the “compact time” variable, $u = 0.1$ and $u = 0.3$. The behavior of the parameter $1 - \lambda(0)$ as function of a is shown in the insertion. Maxima of $1 - \lambda(0)$ correspond to the states which are closest to the symmetric two-Fock states, whereas minima are observed for the ECS’s closest to the single-Fock states. The dependence of the “purity” on a has several distinct “plateaus”, which correspond to the approximate single-Fock states. The “steps” between “plateaus” happen for approximate two-Fock states. The coherence coefficient shows an inverse behav-

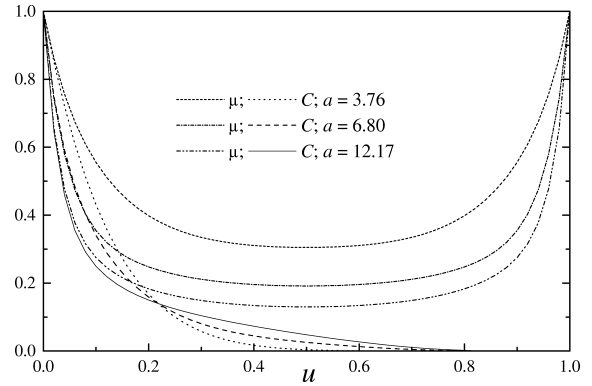


Fig. 5. The “purity” μ and the “coherence” C versus the “compact time” $u \equiv 1 - e^{-2\gamma t}$ for the initial circular state with $N = 8$ and $\nu = 0$ and for three different values of a . The order of the curves from top to bottom (in the left-hand side of the figure): μ for $a = 3.76$; μ for $a = 6.80$; μ for $a = 12.17$; C for $a = 3.76$; C for $a = 6.8$; and C for $a = 12.17$.

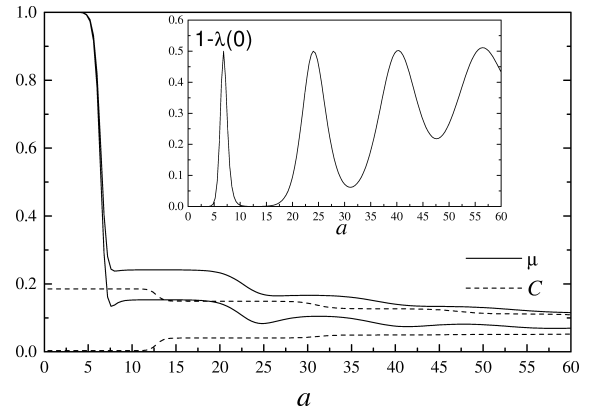


Fig. 6. The “purity” μ and the “coherence” C versus $a = |\alpha_0|^2$ for the initial circular states with $N = 16$ and $\nu = 0$, for two different values of “compact time” u . Solid lines are for μ and dashed lines are for C . Upper curves correspond to $u = 0.1$, lower curves are for $u = 0.3$. In the insertion: the difference $1 - \lambda(0)$ versus a .

ior: the “steps” occur for the approximate single-Fock states.

In Fig. 7 we give the time evolution of the probability distribution function P_n for the initial state $|\tilde{\psi}_N(a)\rangle$ with $N = 8$, $a = 24$ and for $\nu = 0$, at the initial and two intermediary times. One sees that the initial three dominant Fock-state components (black circles) loose their important contribution for the state $|\tilde{\psi}_N\rangle$ as time goes by.

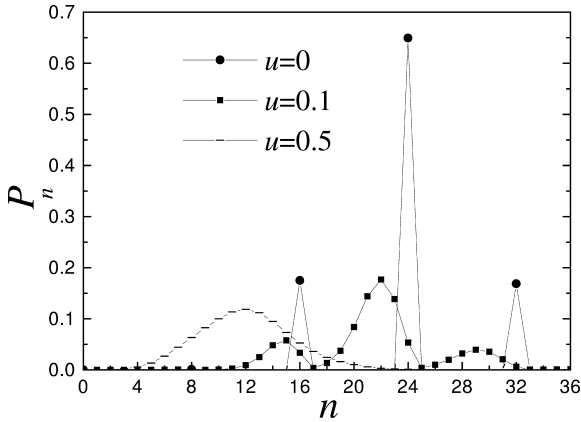


Fig. 7. Time evolution of the probability distribution function P_n for the initial state $|\tilde{\psi}_N(a)\rangle$ with $N = 8$, $a = 24$ and for $\nu = 0$. Black circles stand for the initial state, squares for the “time” $u = 0.1$ and traces for $u = 0.5$.

4. Summary and conclusions

Here we studied and analyzed some interesting properties of the so-called *even circular states*: depending on the number N of coherent states superposition $|\alpha_k\rangle$ and the squared modulus $a = |\alpha_k|^2$, the interference in phase space makes the ECSs very close to either the vacuum state $|0\rangle$, the single-Fock state $|(j+1)N\rangle$ or as two-Fock states superpositions, $|Nj\rangle + |N(j+1)\rangle$, with $j = 0, 1, 2, \dots$. We also give the estimated probabilities for producing such states in a trapped ion with a few laser pulses, specifically for the motion of its center of mass. More interesting is the production of the two-Fock states, where the states may differ by a substantial amount of quanta, as for instance $|8\rangle + |16\rangle$ (with appreciable 12% probability to be produced within the scheme proposed in [14]), which may be viewed as a kind of Schrödinger “cat state”. These states arise from the superposition of N coherent states, differently from the more familiar even and odd “cat states” made of two coherent states $(|\alpha\rangle \pm |-\alpha\rangle)$. Moreover, the two-Fock states constitute a reduction of center of mass motion of the trapped ion to just a two-level system whose gap may be adjusted at wish by an experimentalist, by increasing the number of laser pulses. We complemented our analysis by studying the time evolution after the production of these special states, when the environment acts leading to decoherence and relaxation.

Acknowledgements

A.L.S.S. and S.S.M. acknowledge partial financial support from CAPES and CNPq (Brasília, DF, Brazil), respectively. V.V.D. acknowledges full support from CNPq.

References

- [1] K. Vogel, V.M. Akulin, W.P. Schleich, Phys. Rev. Lett. 71 (1993) 1816; A.S. Parkins, P. Marte, P. Zoller, H.J. Kimble, Phys. Rev. Lett. 71 (1993) 3095; C.K. Law, J.H. Eberly, Phys. Rev. Lett. 76 (1996) 1055.
- [2] S. Haroche, Nuovo Cimento B 110 (1995) 545; L. Davidovich, Rev. Mod. Phys. 68 (1996) 127.
- [3] D.M. Meekhof, C. Monroe, B.E. King, W.M. Itano, D.J. Wineland, Phys. Rev. Lett. 76 (1996) 1796; J.I. Cirac, A.S. Parkins, R. Blatt, P. Zoller, Adv. At. Mol. Opt. Phys. 37 (1996) 237; D.J. Wineland, C. Monroe, W.M. Itano, D. Leibfried, B.E. King, D.M. Meekhof, J. Res. Natl. Inst. Stand. Technol. 103 (1998) 259.
- [4] J.I. Cirac, R. Blatt, A.S. Parkins, P. Zoller, Phys. Rev. Lett. 70 (1993) 762; P. Domokos, J. Janszky, P. Adam, Phys. Rev. A 50 (1994) 3340; L. Davidovich, M. Orsag, N. Zagury, Phys. Rev. A 54 (1996) 5118; R.L. de Matos Filho, W. Vogel, Phys. Rev. Lett. 76 (1996) 4520; H. Moya-Cessa, P. Tombesi, Phys. Rev. A 61 (2000) 025401.
- [5] J. Janszky, P. Domokos, P. Adam, Phys. Rev. A 48 (1993) 2213.
- [6] Z. Bialynicka-Birula, Phys. Rev. 173 (1968) 1207.
- [7] V.V. Dodonov, I.A. Malkin, V.I. Man’ko, Physica 72 (1974) 597.
- [8] B. Yurke, D. Stoler, Phys. Rev. Lett. 57 (1986) 13.
- [9] J. Janszky, P. Domokos, S. Szabó, P. Adam, Phys. Rev. A 51 (1995) 4191.
- [10] M.J. Gagen, Phys. Rev. A 51 (1995) 2715; A. Napoli, A. Messina, Eur. Phys. J. D 5 (1999) 441; M.M. Nieto, D.R. Truax, Opt. Commun. 179 (2000) 197; C. Quesne, Phys. Lett. A 272 (2000) 313.
- [11] R. Ragi, B. Baseia, S.S. Mizrahi, J. Opt. B 2 (2000) 299.
- [12] S. Szabó, P. Adam, J. Janszky, P. Domokos, Phys. Rev. A 53 (1996) 2698.
- [13] S.B. Zheng, G.C. Guo, Eur. Phys. J. D 1 (1998) 105; S.B. Zheng, Opt. Commun. 170 (1999) 67; S.B. Zheng, X.W. Zhu, M. Feng, Phys. Rev. A 62 (2000) 033807.
- [14] W.D. José, S.S. Mizrahi, J. Opt. B 2 (2000) 306.
- [15] A.O. Caldeira, A.J. Leggett, Phys. Rev. A 31 (1985) 1059; D.F. Walls, G.J. Milburn, Phys. Rev. A 31 (1985) 2403;

- C.M. Savage, D.F. Walls, *Phys. Rev. A* 32 (1985) 2316;
V. Bužek, A. Vidiella-Barranco, P.L. Knight, *Phys. Rev. A* 45 (1992) 6570;
W.H. Zurek, S. Habib, J.P. Paz, *Phys. Rev. Lett.* 70 (1993) 1187;
M.R. Gallis, *Phys. Rev. A* 53 (1996) 655;
L. Davidovich, M. Brune, J.M. Raimond, S. Haroche, *Phys. Rev. A* 53 (1996) 1295;
G.S. Agarwal, *Phys. Rev. A* 59 (1999) 3071;
J.P. Paz, W.H. Zurek, *Phys. Rev. Lett.* 82 (1999) 5181;
A. Isar, A. Sandulescu, W. Scheid, *Phys. Rev. E* 60 (1999) 6371;
C.J. Myatt, B.E. King, Q.A. Turchette, C.A. Sackett, D. Kielpinski, W.M. Itano, C. Monroe, D.J. Wineland, *Nature* 403 (2000) 269;
P. Marian, T.A. Marian, *Eur. Phys. J. D* 11 (2000) 257.
- [16] V.V. Dodonov, S.S. Mizrahi, A.L. Souza Silva, *J. Opt. B* 2 (2000) 271.
- [17] D. Stoler, *Phys. Rev. D* 4 (1971) 2309;
J. Katriel, A.I. Solomon, G. D'Ariano, M. Rasetti, *Phys. Rev. D* 34 (1986) 2332;
C.V. Sukumar, *J. Mod. Opt.* 36 (1989) 1591;
V. Bužek, I. Jex, T. Quang, *J. Mod. Opt.* 37 (1990) 159;
J. Sun, J. Wang, C. Wang, *Phys. Rev. A* 46 (1992) 1700;
P. Shanta, S. Chaturvedi, V. Srinivasan, G.S. Agarwal, C.L. Mehta, *Phys. Rev. Lett.* 72 (1994) 1447;
M.M. Nieto, D.R. Truax, *Phys. Lett. A* 208 (1995) 8.
- [18] L. Mandel, *Opt. Lett.* 4 (1979) 205.
- [19] D. Stoler, B.E.A. Saleh, M.C. Teich, *Opt. Acta* 32 (1985) 345.
- [20] D.T. Pegg, L.S. Phillips, S.M. Barnett, *Phys. Rev. Lett.* 81 (1998) 1604.
- [21] M. Hillery, R.F. O'Connell, M.O. Scully, E.P. Wigner, *Phys. Rep.* 106 (1984) 121.
- [22] H.J. Groenewold, *Physica* 12 (1946) 405.
- [23] Yu.L. Klimontovich, *Dokl. Akad. Nauk SSSR* 108 (1956) 1033;
W. Schleich, D.F. Walls, J.A. Wheeler, *Phys. Rev. A* 38 (1988) 1177.
- [24] W. Weidlich, F. Haake, *Z. Phys.* 185 (1965) 30;
M.O. Scully, W.E. Lamb, *Phys. Rev.* 159 (1967) 208.
- [25] I.S. Gradshteyn, I.M. Ryzhik, *Tables of Integrals, Series and Products*, Academic Press, New York, 1994.
- [26] K. Shimoda, H. Takahasi, C.H. Townes, *J. Phys. Soc. Jpn.* 12 (1957) 686;
B.Ya. Zel'dovich, A.M. Perelomov, V.S. Popov, *Zh. Eksp. Teor. Fiz.* 55 (1968) 589, *Sov. Phys. JETP* 28 (1969) 308.